



# Use of agro-industrial residues of plantain (*Musa paradisiaca*) in the adsorption of Ni (II)

## Uso de residuos agroindustriales de plátano (*Musa paradisiaca*) en la adsorción de Ni (II)

Candelaria Tejada-Tovar <sup>1</sup>, Ángel Villabona-Ortiz <sup>1</sup>, Walter Cortina-Góngora <sup>1</sup>, Betty Díaz Navarro <sup>1</sup>, Rodrigo Ortega-Toro <sup>2\*</sup>

<sup>1</sup>Grupo de Investigación Diseño de procesos y aprovechamiento de Biomásas IDAB, Universidad de Cartagena. Avenida del Consulado Calle 30 # 48-152. C. P. 130015. Cartagena de Indias, Colombia.

<sup>2</sup>Grupo de Investigación Food Packaging and Shelf Life FP&SL y Grupo de Investigación Ingeniería de Fluidos Complejos y Reología de Alimentos IFCRA, Universidad de Cartagena, Avenida del Consulado Calle 30 # 48-152. C. P. 130015. Cartagena de Indias, Colombia.

### CITE THIS ARTICLE AS:

C. Tejada, A. Villabona, W. Cortina, B. Díaz and R. Ortega. "Use of agro-industrial residues of plantain (*Musa paradisiaca*) in the adsorption of Ni (II)", *Revista Facultad de Ingeniería Universidad de Antioquia*, no. 103, pp. 138-151, Apr-Jun 2022. [Online]. Available: <https://www.doi.org/10.17533/udea.redin.20210428>

### ARTICLE INFO:

Received: June 24, 2020  
Accepted: April 22, 2021  
Available online: April 22, 2021

### KEYWORDS:

Waste treatment; agricultural wastes; modelling; thermodynamics

Tratamiento de residuos; residuos agrícolas; modelado; termodinámica

**ABSTRACT:** The presence of heavy metals in aqueous media represents a severe threat to ecosystems because they are non-biodegradable, toxic, and carcinogenic. In the present work, the utilization of agro-industrial residues from obtaining plantain starch for removing Ni (II) was studied, establishing the effect of temperature, adsorption dose, and initial concentration. The kinetics, equilibrium, and thermodynamic parameters that determine the process were studied. For this purpose, tests were carried out in a batch system maintaining constant stirring (200 rpm), pH (2), and solution volume (100 mL). The remaining metal concentration was determined by atomic adsorption at 237 nm. It was found that the best adsorption conditions were given at 55 °C, 0.6775 g, and 368 mg/L obtaining a maximum adsorption capacity of 47.57 mg/g corresponding to a removal of 87%. The kinetic model that best fits the experimental data was a pseudo-second-order model, and the isotherm that describes the process is Langmuir and Freundlich, so the adsorption is given by chemisorption and multilayers. The thermodynamic parameters determined suggest that the process is favourable, not spontaneous, endothermic, and irreversible under the studied conditions. The results show that the residual biomass from the obtaining of plantain starch is a good precursor for absorbing Ni (II) in an aqueous solution.

**RESUMEN:** La presencia de metales pesados en medios acuosos representa una grave amenaza para los ecosistemas porque no son biodegradables, además son tóxicos y cancerígenos. En el presente trabajo se estudió la utilización de residuos agroindustriales de la obtención de almidón de plátano para remoción de Ni (II), estableciendo el efecto de la temperatura, dosis de adsorción y concentración inicial. Se estudió la cinética, el equilibrio y los parámetros termodinámicos que determinan el proceso. Para ello, las pruebas se realizaron en un sistema discontinuo manteniendo constante agitación (200 rpm), pH (2) y volumen de solución (100 mL). La concentración de metal restante se determinó mediante adsorción atómica a 237 nm. Se encontró que las mejores condiciones de adsorción se dieron a 55 °C, 0,6775 g y 368 mg / L obteniendo una capacidad máxima de adsorción de 47,57 mg / g correspondiente a una remoción del 87%. El modelo cinético que mejor se ajusta a los datos experimentales fue el de pseudo segundo orden, y la isoterma que describe el proceso es Langmuir y Freundlich, por lo que la adsorción viene dada por quimisorción y multicapas. Los parámetros termodinámicos determinados sugieren que el proceso es favorable, no espontáneo, endotérmico e irreversible en las condiciones estudiadas. Los resultados muestran que la biomasa residual de la obtención de almidón de plátano es un buen precursor para absorber Ni (II) en solución acuosa.

\* Corresponding author: Rodrigo Ortega Toro

E-mail: [rortegap1@unicartagena.edu.co](mailto:rortegap1@unicartagena.edu.co)

ISSN 0120-6230

e-ISSN 2422-2844

## 1. Introduction

The dumping of heavy metal-contaminated effluents into water bodies is one of the most severe environmental

problems in recent years [1]. Heavy metals such as cadmium, chromium, lead, zinc, and nickel discharged into water sources can accumulate in flora and fauna, other organisms and eventually reach the human food chain causing various health problems [2]. Nickel is used in several applications, such as electroplating, dyeing, battery manufacturing, tanneries, paint formulation, ceramic and porcelain glazing, among others [3].

Nickel is not biodegradable and is particularly harmful to humans and other organisms, even in minimal concentrations; it can cause dermatitis, long-term exposure to high doses of nickel can lead to kidney and lung damage, pulmonary fibrosis, gastrointestinal failure, renal oedema, gastrointestinal disorder, cancer and teratogenicity [4]. Besides, nickel carbonyl that is easily absorbed into the skin has been reported to be lethal in humans at atmospheric exposure of 30 mg/L per 30 min [5]. The US-EPA established a maximum concentration of 0.5 mg/L of nickel in drinking water [6]; therefore, the treatment of effluents contaminated with this metal is a priority.

The development of technologies for removing heavy metals is a challenge because conventional techniques such as electrochemistry, membrane treatments, oxidation, precipitation, and heterogeneous photocatalysis are expensive due to the operating costs and reagents required [7]. Thus, bio-adsorption is presented as an economical and environmentally friendly alternative, which allows the recovery of waste as contaminant adsorbents due to the presence of active centres in its lignocellulosic structure [8]. Different biomasses have been used to remove heavy metals such as lychee [9], orange [10], *Pisum sativum* [11], yam [12], lime [13], cranberry seed peel, rosehip seed peel, and banana peel [14], rambutan peels [15], macauba [16], sweet lime and lemon peel powder [17], which reported good yields and adsorption capacity.

On the other hand, more than 102 million plantains are produced annually, with 35% of each fruit producing approximately 36 million tons of waste after its exploitation [18]. In Colombia, a large number of *Musa paradisiaca* plantain crops in the department of Bolívar have generated a significant increase in post-harvest waste because their production is focused on marketing or as a household food option. After selecting the fruit with the best conditions, those that do not meet market demands in terms of size and plantain maturity are used as fertilizer for the harvest through decomposition, representing 10% of the total plantain crop produced. Therefore, in this research, the residual biomass of the plantain starch production process is proposed as a nickel Ni (II) bio-adsorbent in solution in a batch system, evaluating the effect of temperature,

adsorbent dose, and concentration of the material in the adsorption.

This work provides the process operating conditions for implementing the Ni (II) removal method by biosorption, as an efficient technology, easy to implement, and friendly to the environment, simultaneously solving the disposal and use of large volumes of agro-industrial residues from plantain. This topic contributes to the state of the art of the subject of clean technologies because it presents an efficient alternative, with low energy consumption and without chemical reagents; therefore, it can be considered a low cost and easy to implement solution. These previous results contribute to the applied engineering literature for the implementation of the technology on a pilot scale with real wastewater. It also highlighted a contribution to studying the agro-industrial waste from the process of obtaining plantain starch, which is part of a series of studies for the implementation of a biorefinery for processing various agricultural products of the Caribbean region, such as yam, yucca, and plantain. It is projected to process and obtain starch from these three raw materials, to establish a bio adsorbent production line taking advantage of the waste from this process.

## 2. Methodology

### 2.1 Experimental design

An experimental design following a continuous linear factor on central compound response surface, star, was developed in the Statgraphics Centurion XVI.II. Software. In Table 1, the experimental ranges and levels of variation of the variables are shown. In Table 1, the experimental ranges and levels of variation of the variables are shown.

### 2.2 Preparation of the bio-sorbent and the synthetic solution

Post-harvest plantain waste was obtained in the municipality of Santa Catalina de Alejandría in the department of Bolívar (Colombia). The residual biomass of plantain starch was obtained as proposed by Maniglia and Tapia-Blácido [19]. Initially, the fruit was peeled, cut, washed with distilled water, and dipped in a 0.25% NaOH solution; the mixture was refrigerated for 18 h, reduced in size, filtered. Subsequently, the residual bagasse was adjusted to 7 and dried at 40 °C to a constant mass. The residual biomass was sieved in an Edibon Orto Alresa Vibro sieve shaker.

A Ni (II) base solution was prepared at 1000 mg/L using Merk Millipore analytical grade nickel sulphate (NiSO<sub>4</sub>); 4.479 g of reagent was added to 1 L of deionized water.

**Table 1** Experimental design

| Independent variables | Units | Range and level |       |       |     |           |
|-----------------------|-------|-----------------|-------|-------|-----|-----------|
|                       |       | $-\alpha$       | -1    | 0     | +1  | $+\alpha$ |
| Temperature           | °C    | 30              | 40    | 55    | 70  | 80        |
| Amount of adsorbents  | g     | 0.135           | 0.355 | 0.678 | 1   | 1.22      |
| Initial concentration | mg/L  | 31.82           | 100   | 200   | 300 | 368.179   |

The solution was then diluted to reach the concentrations in Table 1.

## 2.3 Adsorption tests

The Ni (II) adsorption tests were performed individually in a Gemmy Industrial brand IN-666 shaker incubator. For this purpose, 100 mL of solution were taken at pH 6 and 200 rpm for 24 h, following the design of experiments in Table 1 [20]. The remaining metal concentration in the solution was determined by atomic adsorption at 232 nm. Adsorption efficiency and capacity were determined according to Equations 1 and 2:

$$\%E = \frac{C_i - C_f}{C_i} * 100 \quad (1)$$

$$q_t = \frac{(C_i - C_f) * V}{m} \quad (2)$$

Where  $q_t$  (mg/g) is the adsorption capacity,  $\%E$  is the adsorption efficiency,  $C_i$  (mg/L) is the initial concentration,  $C_f$  (mg/L) is the final concentration,  $m$  (g) is the mass of the adsorbent, and  $V$  (L) is the volume of the solution.

## 2.4 Kinetics and adsorption isotherms

Kinetics studies were performed at the best experimental conditions of temperature, adsorbent dose, and initial concentration using 100 mL of solution, at pH (6) and 200 rpm. The samples were placed in the orbital shaker, and aliquots were taken at each time interval (5, 10, 15, 20, 30 min, 1, 2, 4, 8 and 22 h) to determine the behaviour of the contaminant over time [21]. The experimental data were fitted to the pseudo-first-order, pseudo-second-order, and Elovich models. Adsorption isotherms were performed by varying the initial concentration of the contaminant (50, 100, 200, and 300 mg/L) to determine its influence on the process as it reached equilibrium. The experimental data were adjusted to the Langmuir and Freundlich models. The kinetic and isothermal fitting models are shown in Table 2.

## 2.5 Thermodynamic study

The graphical method based on the Van't Hoff equation was used to determine the spontaneity, type of adsorption, and to predict the magnitude of changes on the surface

of the adsorbent, respectively. Therefore, the change in Gibbs' standard free energy ( $\Delta G$ ), enthalpy ( $\Delta H$ ), and entropy ( $\Delta S$ ) were estimated by testing the percentage removal of the samples at 33.8, 40, 55, 70, and 76.2 °C. Then the final concentration of the metal after adsorption was determined, and the amount of metal removed was estimated. Subsequently, an Ln ( $K_c$ ) vs.  $T^{-1}$  graph was made, and the thermodynamic parameters were determined [23]. The thermodynamic parameters mentioned were calculated according to Equations 3, 4, and 5.

$$K_C = \frac{Q_T}{C_T} \quad (3)$$

$$\Delta G = -RT * \ln K_C \quad (4)$$

$$\ln K_C = \frac{-\Delta H^\circ}{RT} + \frac{\Delta S^\circ}{R} \quad (5)$$

## 3. Results

### 3.1 Characterization of the biomaterial

The elemental characterization showed that carbon with 47.74% was the element with the highest content in the residual starch biomass, followed by oxygen and hydrogen. The results of the elemental analysis are shown in Table 3.

The chemical analysis presented in Table 4 shows that the high presence of carbons, oxygen and hydrogen in the biomass indicated in Table 3 is due to the 41.80% content of cellulose. Lignin and hemicellulose are present to a lesser degree. The high content of cellulose and lignin in the bio-sorbent under study corresponds to the presence of carbon and oxygen from the elemental analysis. The existence of these compounds in bio-sorbents with lignocellulosic origin offers active centres for the union of metallic ions because of the appearance of the hydroxyl group in the material's structure. Consequently, the material under study is massively useful when applied in the process of adsorption of metallic ions due to the cationic nature of these contaminants [24, 25].

The Fourier Transform Infrared Spectroscopy (FTIR) technique was used before and after Ni (II) adsorption (Figure 1), in order to determine the functional groups present in the biomaterial that could be involved in the

**Table 2** Kinetic and isothermal models

| Model               | Equation   | Parameters   |
|---------------------|--|--|
| Pseudo-first-order  | $q_t = q_{e1} (1 + e^{-k_1 t})$  | $k_1$ ( $\text{min}^{-1}$ ): Lagergren constant<br>$q_{e1}$ (mg/g): adsorption capacity in the equilibrium<br>$q_t$ (mg/g): adsorption capacity for a time $t$<br>$t$ : time   |
| Pseudo-second-order | $q_t = \frac{t}{\left(\frac{1}{k_2 q_{e2}^2}\right) + \frac{t}{q_{e2}}}$ | $k_2$ ( $\text{min}^{-1}$ ): second-order adsorption constant<br>$q_{e2}$ (mg/g): adsorption capacity in the equilibrium<br>$q_t$ (mg/g): adsorption capacity for a time $t$<br>$t$ : time   |
| Elovich             | $a_t = \alpha * \ln(\alpha * \beta) + \alpha * \ln t$                    | $q_t$ (mg/g): is the adsorption capacity for a time $t$<br>$\alpha$ (mg/g.min <sup>-1</sup> ): initial rate of adsorption<br>$\beta$ (g/mg): is the desorption constant related to the surface extent  |
| Freundlich          | $q_e = k_f * C_e^{1/n}$  | $q_e$ (mg/g): is the amount of metal adsorbed in the balance<br>$C_{eq}$ (mg.L <sup>-1</sup> ): is the residual concentration of the metal in solution at equilibrium<br>$K_f$ (mg/g)(mg/L): and $n$ is a measure of the adsorption intensity  |
| Langmuir            | $q_e = q_{max} \frac{K_L C_f}{1 + K_L C_f}$                              | $q_e$ (mg/g): is the amount of adsorbate retained in the adsorbent in the equilibrium<br>$C_f$ (mg/L): is the residual concentration of the metal in the equilibrium<br>$q_{max}$ (mg/g): is the maximum adsorption corresponding to the saturation sites<br>$K_L$ (L/mg): is the relationship between the adsorption/desorption rates |

Source: Adapted from [22]

**Table 3** Elemental analysis of residual plantain biomass

| Element content (%) | Value | Methods     |
|---------------------|-------|-------------|
| Sulphur             | 0.37  | AOAC 975.53 |
| Carbon              | 47.74 | AOAC 949.12 |
| Hydrogen            | 15.27 | AOAC 949.12 |
| Nitrogen            | 0.58  | AOAC 984.13 |
| Oxygen              | 23.98 | AOAC 963.29 |

**Table 4** Chemical analysis of residual plantain biomass

| Compound content (%) | Value | Method                      |
|----------------------|-------|-----------------------------|
| Lignin               | 26.22 | TAPPI T 222 om-83           |
| Cellulose            | 41.80 | TAPPI T 203 os-74           |
| Hemicellulose        | 15.81 | holocellulose and cellulose |

ion exchange between the adsorbent and the metal. The IR spectrum of the residual plantain biomass before the adsorption process registers vibrations at wavelengths between 3000 and 3500  $\text{cm}^{-1}$ , indicating the presence of hydroxyl (-OH) functional groups; between 3200 and 3500  $\text{cm}^{-1}$  is observed the appearance of amines and small

carbonyl overtone signals due to the stretching vibrations of the -OH link [25]. The possible disturbances of C-H methyl, methylene, and methoxy groups are given by the peak of 2927.94  $\text{cm}^{-1}$  [26]. Wavelengths between 2000 and 2500  $\text{cm}^{-1}$  show slight signals of alkynes and carboxylic acids [27].

Additionally, the FTIR spectrum has bands close to 1650  $\text{cm}^{-1}$  that indicate the existence of functional groups of cellulose, hemicellulose, and lignin due to the stretching of C=O and C-O by vibrations of carboxyl groups of hemicellulose and lignin [28, 29]. This fact indicates the strong presence of aromatic rings produced by hydrogen vibrations representing the stretching of C=C. Between 1000 and 1200  $\text{cm}^{-1}$ , it is evident the presence of primary, secondary, and tertiary alcohols, a product of the stretching vibrations of the C-OH bond, and the flexions between the plane (1225-950  $\text{cm}^{-1}$ ) are only complementary signals because of the C-C, C-N, and C-O stretch fall in the same region. Also, several signals appear depending on the hydrogen content, which could affect the interactions that rule the adsorption phenomena when the adsorbate interacted with the carbonyl groups or surface alkenes of the bio-sorbent [29]. The presence of the above-mentioned functional groups in the 400-4000

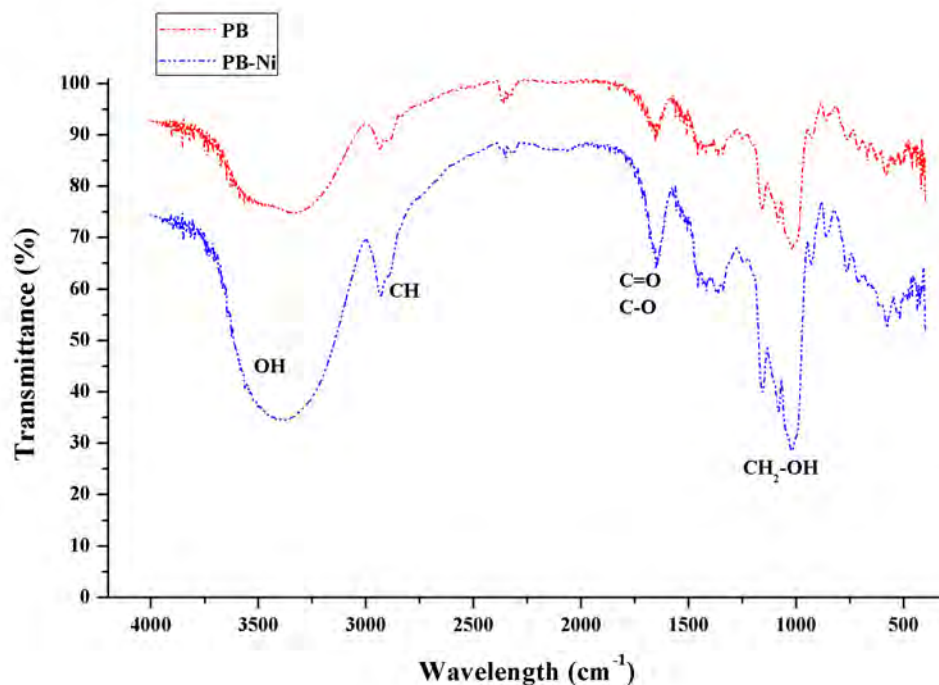


**Figure 1** IR spectrum of plantain biomass before and after Ni (II) adsorption

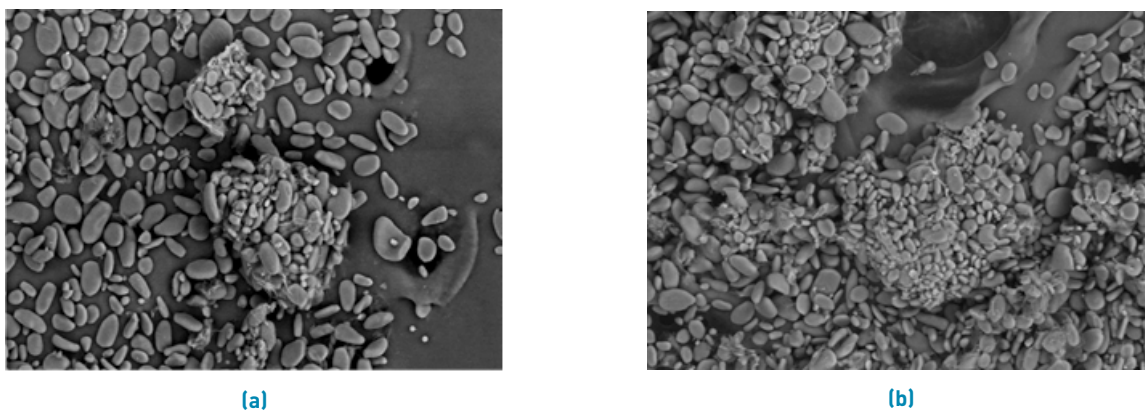


**Figure 2** SEM microphotographs of residual plantain biomass (a) before and (b) after Ni adsorption (II)

$\text{cm}^{-1}$  spectrum is attributed to the high content of lignin, cellulose, and hemicellulose in the structure of the bio-sorbent extracted from the residual biomass from plantain starch [30].

The infrared spectrum after ion removal shows a remarkable increase in the width of the spectral bands after the Ni (II) adsorption process. Spectrum changes were observed in the  $1000 \text{ cm}^{-1}$  band due to bond N-H bending and a shift towards a lower band. Therefore, it is concluded that the nitrogen atom should be the leading adsorption site for Ni (II) binding in the biomass. Furthermore, changes in the FTIR spectrum at wavelengths  $3500\text{-}3408.0 \text{ cm}^{-1}$  and  $1100.3\text{-}1090.4 \text{ cm}^{-1}$

can also be assigned to the stretching vibration in the OH groups and the C-O stretching vibration, respectively [31]. Another significant change in transmittance is observed in the wavenumber  $2904.6\text{-}2835.2 \text{ cm}^{-1}$  after the adsorption. This is attributed to the C-H methyl, methylene, and methoxy groups vibrations present in the biomass. The above is consistent with the results obtained by different authors [32].

Figure 2 shows the SEM micrographs at a magnification of 200x of the residual plantain starch biomasses before (Figure 2a) and after Ni (II) adsorption (Figure 2b). A smooth surface structure is shown, with small beads that are attributed to the presence of lignin, hemicellulose, and

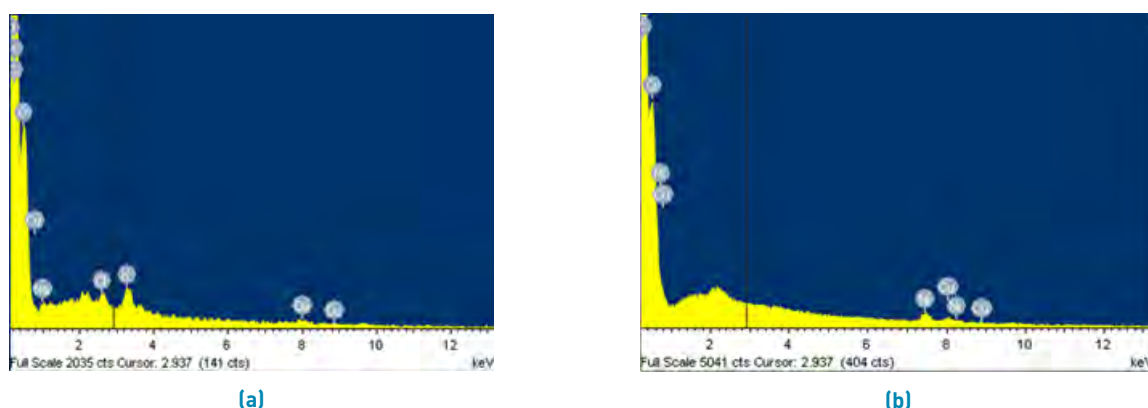


**Figure 3** EDS spectra of residual biomass of plantain (a) before and (b) after Ni (II) adsorption

**Table 5** Results of Ni (II) adsorption capacity on residual biomass of plantain starch

| Adsorbent dosage (g) | T (°C) | C <sub>i</sub> (mg/L) | C <sub>f</sub> (mg/L) | %E    | q <sub>t</sub> (mg/g) |
|----------------------|--------|-----------------------|-----------------------|-------|-----------------------|
| 0.6775               | 55     | 200                   | 142.99                | 28.50 | 8.41                  |
| 0.355                | 70     | 300                   | 150.55                | 49.81 | 42.10                 |
| 1                    | 40     | 100                   | 26.50                 | 73.49 | 7.35                  |
| 0.6775               | 55     | 31.82                 | 15.16                 | 52.36 | 2.46                  |
| 0.355                | 40     | 300                   | 145.44                | 51.52 | 43.54                 |
| 0.14                 | 55     | 200                   | 155.94                | 22.03 | 32.61                 |
| 0.355                | 40     | 100                   | 34.22                 | 65.77 | 18.53                 |
| 0.6775               | 80.22  | 200                   | 98.26                 | 50.87 | 15.02                 |
| 1                    | 70     | 100                   | 29.56                 | 70.43 | 7.04                  |
| 1.22                 | 55     | 200                   | 78.77                 | 60.62 | 9.94                  |
| 1                    | 40     | 300                   | 125.06                | 58.31 | 17.49                 |
| 0.6775               | 30     | 200                   | 90.88                 | 54.56 | 16.11                 |
| 0.355                | 70     | 100                   | 32.78                 | 67.21 | 18.93                 |
| 0.6775               | 55     | 368.179               | 45.89                 | 87.53 | 47.57                 |
| 1                    | 70     | 300                   | 144.63                | 51.79 | 15.54                 |
| 0.6775               | 55     | 200                   | 142.99                | 28.50 | 8.41                  |

T: Temperature, C<sub>i</sub>: Initial concentration, C<sub>f</sub>: final concentration, and q<sub>t</sub>: adsorption capacity.

cellulose [33]. In contrast, the plantain starch biomass micrographs after Ni (II) adsorption are shown in Figure 2. They exhibit a clearly soft and porous structure. The presence of pores and cavities on the surface is equivalent to the increased surface area accessible for adsorption. It can be observed that there is no precipitation of the metal on the surface of the adsorbent. So, it can be said that chelate formation does not appear, and the adsorption occurs by the interaction of electrostatic forces. The adsorption of the ions occurs inside the pores and cavities of the material [34]. These results are consistent with those found when using *Citrus limetta* for adsorption of Ni (II) [35], *Citrus limettioides* [36], coconut sawdust, and bagasse [37]. Previously, we reported for the residual biomass of plantain starch a surface area of 3.859 m<sup>2</sup>/g, a pore volume of 4 × 10<sup>-7</sup> m<sup>3</sup>/g, and pore size of 4.89 × 10<sup>-9</sup> m; thus, it can be said that the bio-adsorbent has the presence of mesoporous, with a small volume and surface

area [38].

Figure 3 shows the EDS spectra of the residual plantain biomass before (Figure 3a) and after the removal of Ni (II) (Figure 3b). The EDS showed a high content of oxygen, carbon, and nitrogen, which is consistent with the elemental analysis presented in Table 2, characteristic of biomaterials of lignocellulosic origin. After the adsorption process, the appearance of Ni (II) in the spectrum is observed, confirming the adsorption on the surface of the adsorbent and the disappearance of chlorine, sodium, and potassium, which would be the active centres to which the ion adhered [37, 39].

### 3.2 Adsorption tests

After carrying out the Ni (II) adsorption tests using the residual plantain biomass, the effect of the amount of

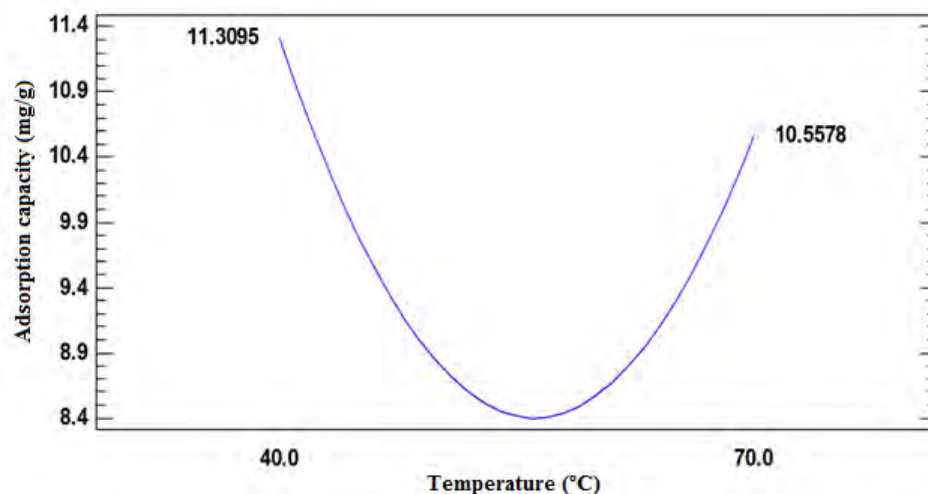


Figure 4 Effect of temperature on Ni (II) adsorption

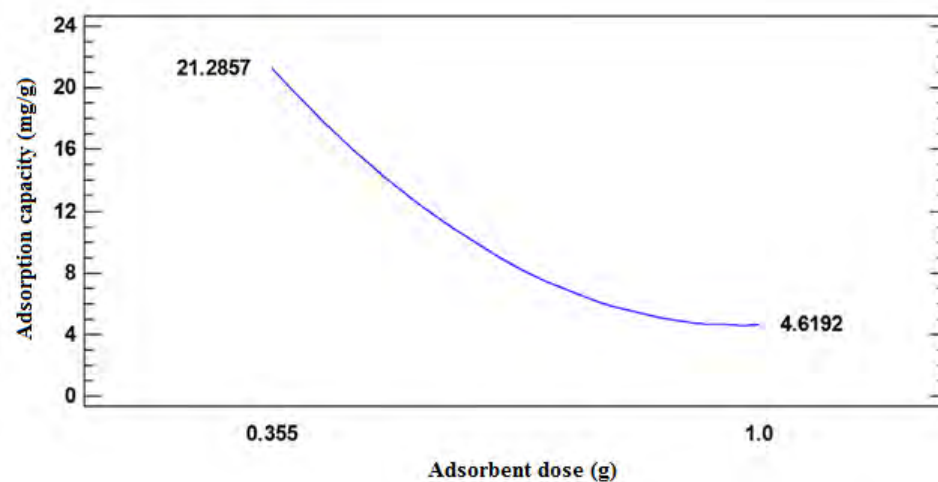


Figure 5 Effect of adsorbent dose on the adsorption capacity of Ni (II)

biomass, the temperature, and the initial concentration of the metal was evaluated by calculating the adsorption capacity of the metal ion. In Table 5, the results in terms of adsorption capacity (Equation 1) and removal efficiency (Equation 2) are shown at the set conditions experimental design.

It was established that it is at 55 °C, 368.2 mg/L and 0.6775 g of biomaterial, where a higher percentage of removal of 87.53 % is obtained.

The temperature effect on the adsorption process is useful in the actual application of the adsorption system, as the effluents are discharged at different temperatures [39]. The effect of temperature on the adsorption capacity is shown in Figure 4.

It is observed that a temperature increase from 40 to 70 °C favours the adsorption of Ni (II) ions, suggesting that the system is endothermic and needs energy supply to increase the electrostatic interaction forces between the active centres of the material and the ions [40]. The favourable effect of temperature on Ni (II) adsorption may be due to the increased ionization of the lignocellulosic components [41]. They act as adsorption sites, thus promoting the increased rate of diffusion of Ni (II) through the outer boundary layer into the pores [42, 43].

The effect of the dose on the adsorption capacity is shown in Figure 5.

A decrease in the adsorption capacity of the metal was observed as the amount of adsorbent increases, with the maximum capacity and percentage of adsorption being

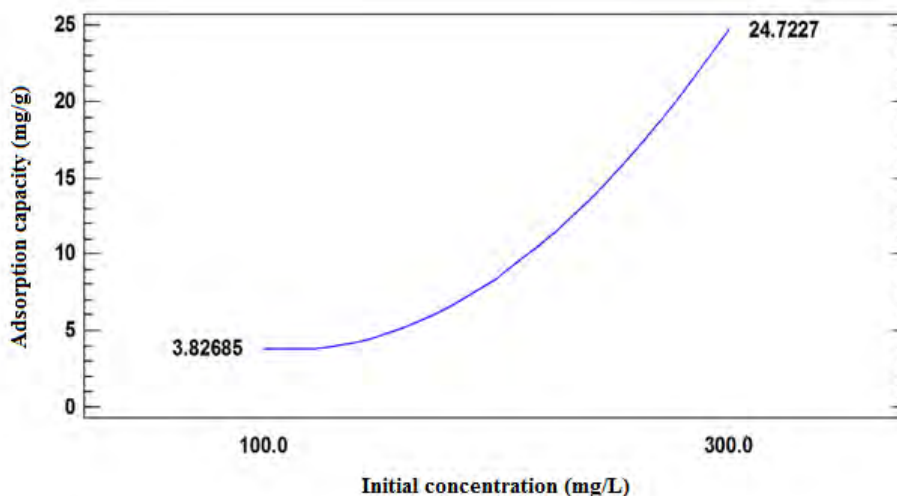


Figure 6 Effect of the initial Ni (II) concentration on the adsorption process

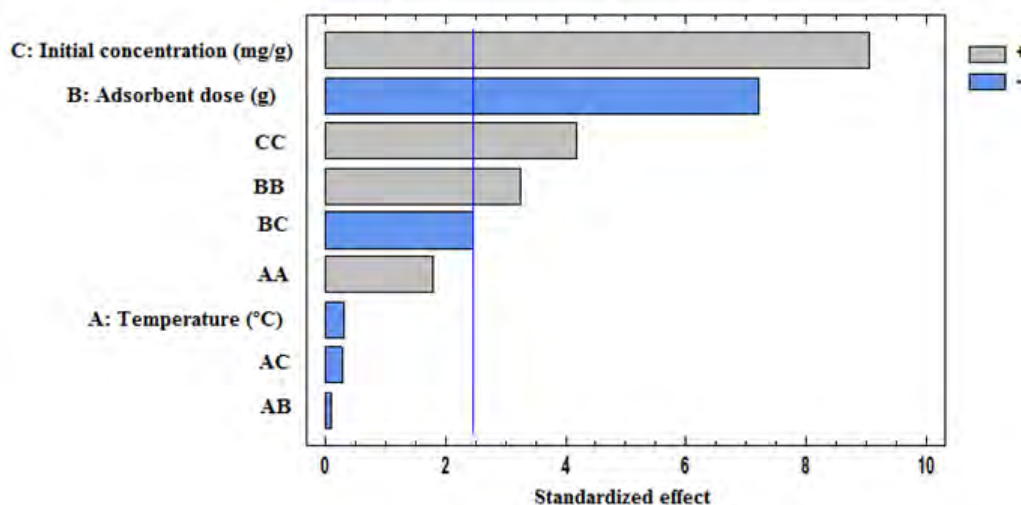


Figure 7 Standardized effect Pareto diagram for Ni (II) adsorption

reached at an adsorbent dose of 0.6775 g. At a high dose of adsorbent, reduction of adsorption capacity may be due to the binding of ions to the active sites and establishment of the balance between ions bound to sorbent and ions in the solution. Therefore, there may be a competition of solute ions for limited available binding sites, electrostatic interactions, overlapping or aggregation of adsorption sites, low surface area, interference between binding sites, and contact of ions below higher adsorbent densities [41].

Figure 6 shows the effect of the initial concentration of Ni (II) on the adsorption capacity of the metal on the bio-sorbent. An increase in adsorption capacity is observed as the concentration of contaminant in solution increases. This event could be due to the higher ionization potential of the metal at higher concentrations and the

increase in the concentration gradient as the driving force promoting mass transfer, thus decreasing the resistance to mass transfer between the bio-sorbent and the bio-sorbent medium [43].

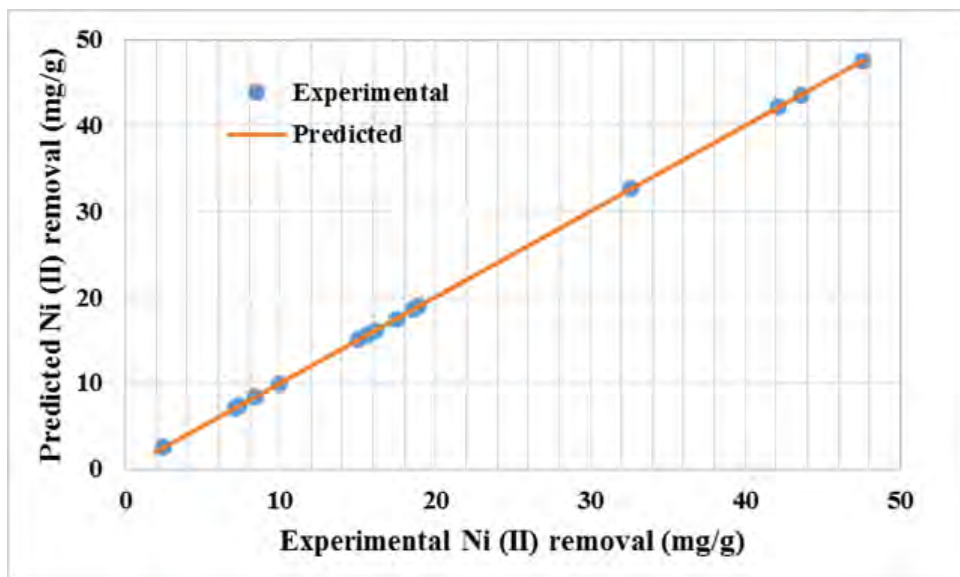
### 3.3 Statistical analysis

Figure 7 shows the standardized Pareto diagram for Ni (II) adsorption capacity, which shows in a standardized way that the most positively influential variable is the initial concentration and the initial concentration-initial concentration interaction. At the same time, the adsorbent dose has a significant negative influence on the process [44].

Likewise, the statistical significance of the second-order equation revealed that the regression is statistically

**Table 6** Analysis of variance for Ni (II) adsorption capacity on residual plantain biomass

| Parameters              | Sum of squares | Gl | Average square | Ratio-F | Value-P |
|-------------------------|----------------|----|----------------|---------|---------|
| Ni (II) Model           | 3031.58        | 15 | 202.105        | 32.13   | 0.0042  |
| C:Initial concentration | 1490.77        | 1  | 1490.77        | 81.79   | 0.0001  |
| T:Temperature           | 1.92938        | 1  | 1.92938        | 0.11    | 0.7560  |
| D:Adsorbent dose        | 948.38         | 1  | 948.38         | 52.03   | 0.0004  |
| CC                      | 318.184        | 1  | 318.184        | 17.46   | 0.0058  |
| CT                      | 1.5138         | 1  | 1.5138         | 0.08    | 0.7829  |
| CD                      | 109.076        | 1  | 109.076        | 5.98    | 0.0500  |
| TT                      | 58.8052        | 1  | 58.8052        | 3.23    | 0.1226  |
| TD                      | 0.18605        | 1  | 0.18605        | 0.01    | 0.9228  |
| DD                      | 190.801        | 1  | 190.801        | 10.47   | 0.0178  |
| Total error             | 109.359        | 6  | 18.2265        |         |         |



**Figure 8** Relationship between predicted and experimental data for Ni (II) adsorption

significant, and based on the results of ANOVA, the regression model of Equation 6, reports a high value of  $R^2$  of 99.39%, which implies a high correlation between observed and predicted values [45, 46].

$$\begin{aligned}
 q_t = & 63.8671 - 0.036C - 1.177T - \\
 & 60.331D + 0.00058C^2 - \\
 & 0.00029CT - 0.1144CD + \\
 & 0.0112T^2 - 0.0315TD + \\
 & 43.6343D^2 \quad (6)
 \end{aligned}$$

Where  $q_t$  (m/g) is the adsorption capacity of the adsorbent,  $C$  (mg/L) is the initial concentration of the contaminant,  $T$  (°C) the temperature and  $D$  (g), and the adsorbent dose. The positive and negative signs before the terms indicate the synergistic and antagonistic effect of the respective variables [47, 48].

To evaluate the individual interaction and the quadratic

effects of the variables that influence the Ni (II) removal capacity on the plantain residues, an analysis of variance (ANOVA) was performed. Table 6 shows the results obtained from the analysis of variance; this table shows the partitions of the adsorption variability for each variable evaluated with a p-value < 0.05. It is observed that the factors with greater relevance in the design are adsorbent dose (g), initial concentration (mg/L), and initial concentration-initial concentration interactions (Figure 7). The ANOVA validated the importance and adequacy of the model obtained by optimizing the response.

Regarding the percentage of Ni (II) removal, from Table 6, it can be seen that the F-value of the model is 32.13 and the P-value of 0.042, which means that the model is statistically significant (Equation 6). The model's significant terms were  $C$ ,  $D$ ,  $CC$ , and  $DD$ , with only  $T$  as a non-significant factor for the response. From the statistical results obtained, it can be seen that the model

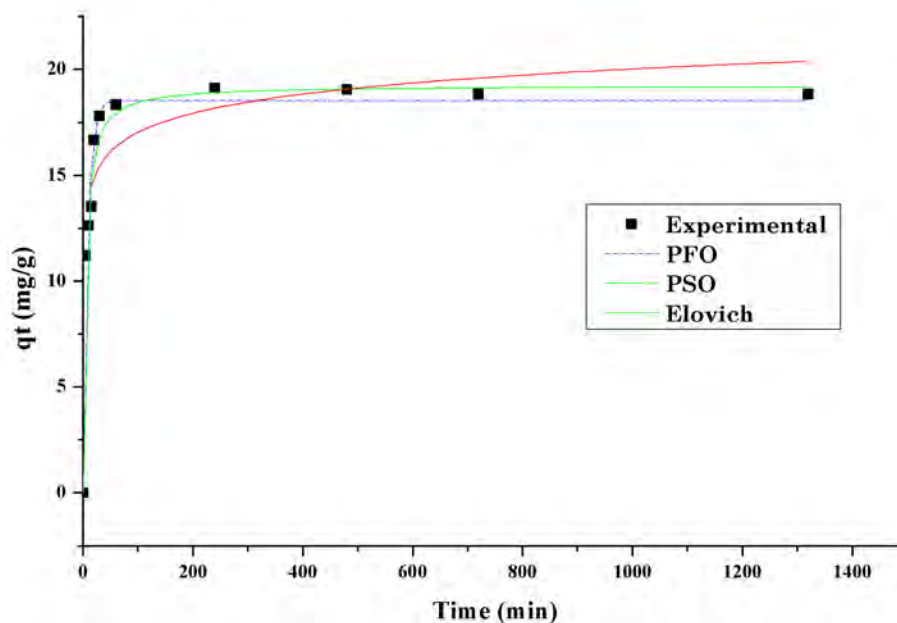


Figure 9 Fitting to Ni (II) adsorption kinetics models

was adequate to predict the removal of Ni (II) within the range of the variables studied. A correlation coefficient between the real data and those predicted by the model of 99.26% was obtained, portraying that the developed models successfully captured the relationship between the variables of the adsorption process evaluated and the response (Figure 8).

It is observed that the most influential variable on the process is the initial concentration of the contaminant. This variable is a driving force for the mass transfer of the metal ion from the solution to the surface of the adsorbent, whereby as the concentration in the solution increases, the process is more efficient. The adsorption capacity will be higher because this is the result of the increasing concentration gradient that acts as a driving force to overcome the resistance to mass transfer of the metal ions between the adsorbate and the adsorbing species [48]. Also, the variation in the percentage of elimination and adsorption capacity of Ni (II) on residual biomass of plantain starch does not have a proportional variation profile, considering that this variable is one of the most significantly influential in the process.

### 3.4 Adsorption kinetics

The kinetic study was carried out to analyse the behaviour of the adsorption process in time. In Figure 9, the kinetics of Ni (II) adsorption and the fit to the pseudo-first-order, pseudo-second-order, Elovich, and intraparticle diffusion adsorption models are shown. It is observed that the rate

of adsorption is fast adsorption in the first 60 min, reaching a maximum metal adsorption capacity of 19.1 mg/g, which is high compared to 9.8 mg/g when using tea residues [49] and 9.13 mg/g on pisum [11]. This rapid rate of biosorption at the beginning of the process can be attributed to the high availability of sorption sites during this period, which demonstrates the effectiveness of residual plantain starch biomass as a bio-sorbent in the short contact time with Ni (II) [4].

The fit parameters of the models used were found by non-linear fit and are shown in Table 7. It was found that the pseudo-second-order model describes better the adsorption kinetics of Ni (II). Figure 8 suggests that two active sites of the biomass can adsorb the metal ion; from the value of the constant  $k_2$ , it is shown that the initial sorption rate for Ni (II) is low, thus also achieving a low adsorption efficiency. Likewise, Elovich's model also presented a good fit according to the correlation coefficient of 0.9299 and the parameter  $\alpha$  of 6806.2044 mg/g min. According to this, it can be concluded that Ni (II) adsorption takes place inside the pores of the particles of the bio-adsorbent materials considering the heterogeneity of the active sites of the adsorbent found in the FTIR spectrum of Figure 1, so they exhibit different activation energies along the adsorption process [29, 50].

### 3.5 Adsorption isotherms

In order to describe the equilibrium of the separated solute between the solid and liquid phases, the evaluation

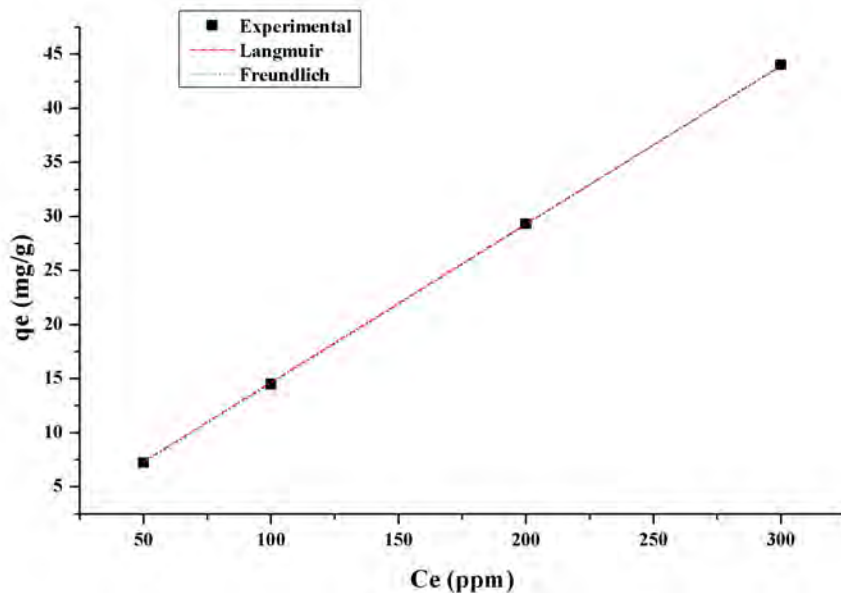


Figure 10 Fitting to isothermal models

Table 7 Adjustment parameters for Ni (II) adsorption kinetics

| Kinetic model | Parameters | Values    |
|---------------|------------|-----------|
| First Order   | $q_{e1}$   | 18.5375   |
|               | $k_1$      | 0.1233    |
|               | $R^2$      | 0.9570    |
| Second Order  | $q_{e2}$   | 19.2432   |
|               | $k_2$      | 0.0122    |
|               | $R^2$      | 0.9815    |
|               | $\beta$    | 0.7726    |
| Elovich       | $\alpha$   | 6806.2044 |
|               | $R^2$      | 0.9299    |

the ions and the active centres are strong, indicating that the process is favourable with high adsorption intensity [44, 52].

Table 8 Adjustment parameters of isothermal models

| Model      | Parameters | Values              |
|------------|------------|---------------------|
| Langmuir   | $q_{max}$  | 27775.5876          |
|            | $b$        | $1.6256 \cdot 10^5$ |
|            | $R^2$      | 0.9998              |
| Freundlich | $K_f$      | 0.1391              |
|            | $1/n$      | 1.0096              |
|            | $n$        | 0.9905              |
|            | $R^2$      | 0.9999              |

of the data obtained in the Ni (II) adsorption process on the residual biomass of plantain starch was carried out, using models such as Langmuir and Freundlich. The adjustment of the equilibrium data by non-linear regression is shown in Figure 10, and the adjustment parameters are shown in Table 8.

It was found that the two models evaluated to fit the Ni (II) adsorption data, which indicates that both mechanisms have an incidence. However, physical forces prevail over them, and the formation of a monolayer limits the process; no desorption reaction is considered. The number of species adsorbed does not exceed the number of active sites [51].

The value of Freundlich's constant  $n$  is in the range 1-10, so the electrostatic interactions and links formed between

### 3.6 Thermodynamic parameters

The thermodynamic study of adsorption allows establishing the mechanisms of the process in terms of reversibility and spontaneity, and its exothermic or endothermic nature, by calculating the change in Gibbs' standard free energy ( $\Delta G^\circ$ ), standard enthalpy ( $\Delta H^\circ$ ) and standard entropy ( $\Delta S^\circ$ ). The thermodynamic parameters mentioned above were calculated by applying Van't Hoff's graphical method and Equations 3 to 5; the results are shown in Table 9.

The positive value of  $\Delta H$  suggests that the process is endothermic and needs energy supply to be able to happen, which confirms the results shown in Figure 4 [53].

**Table 9** Thermodynamic parameters of Ni (II) adsorption

| Temperature (K) | $\Delta G$ (kJ/mol) | $\Delta H$ (kJ/mol) | $\Delta S$ (kJ/mol*K) |
|-----------------|---------------------|---------------------|-----------------------|
| 303.15          | 16.8038             | 2.6449              | -0.04671              |
| 328.15          | 17.9713             |                     |                       |
| 353.15          | 19.1389             |                     |                       |

The negative values of  $\Delta S$  suggest that the biomass has an affinity for the ion and strong bonds are formed on the surface, making the process irreversible; these results confirm what is shown by the FTIR and SEM-EDS analysis, as well as the fit of the equilibrium data to Freundlich's model [54]. The positive values of Gibbs' free energy indicate that the adsorption process is not spontaneous, favourable and that reactions are not feasible at moderate temperatures [52, 55].

## 4. Conclusions

The characterization of the residual plantain biomass shows the presence of hydroxyl, carbonyl, and carboxyl groups belonging to cellulose and lignin, which are attributed to participating in the adsorption process. After the adsorption process, the decrease of the adsorption bands was observed, so the metal removal was proved. The SEM and EDS analysis show that the process occurs due to electrostatic interactions between Ni (II) and the active centres inside the pores of the biomaterial. It was found that the best conditions for the removal of nickel were 368 mg/L, 0.6775 g of adsorbent, and 55 °C, with a yield of 87% and a maximum adsorption capacity of 47.57mg/g. The adsorption kinetics were adjusted to the pseudo-second-order model and the isotherm to the Langmuir and Freundlich models, which suggests that the process is controlled by chemical reaction and occurs in multilayers. The adsorbent under study is presented as a viable and sustainable alternative for the removal of Ni (II) present in aqueous solutions.

## 5. Declaration of competing interest

We declare that we have no significant competing interests including financial or non-financial, professional, or personal interests interfering with the full and objective presentation of the work described in this manuscript.

## 6. Acknowledgements

The authors thank the Universidad de Cartagena for the support to develop this research, laboratories, software, and time of the research professors.

## References

- [1] B. A. Bhanvase, R. P. Ugwekar, and R. B. Mankar, *Novel Water Treatment and Separation Methods: Simulation of Chemical Processes*. Toronto, Waretown, NJ: Apple Academic Press, 2017.
- [2] A. Azimi, A. Azari, M. Rezakazemi, and M. Ansarpour, "Removal of heavy metals from industrial wastewaters: A review," *ChemBioEng Reviews*, vol. 4, no. 1, Feb. 1, 2017. [Online]. Available: <https://doi.org/10.1002/cben.201600010>
- [3] C. Tejada-Tovar, A. Villabona-Ortíz, E. Ruiz-Paternina, A. Herrera-Barros, and R. Ortega-Toro, "Characterization and use of agroindustrial by-products in the removal of metal ions in aqueous solution," *Jurnal Teknolog (Sciences & Engineering)*, vol. 81, no. 6, Nov. 2019. [Online]. Available: <https://doi.org/10.11113/jt.v81.13644>
- [4] Y. F. Lam, L. Yee, S. J. Chua, S. S. Lim, and S. Gan, "Insights into the equilibrium, kinetic and thermodynamics of nickel removal by environmental friendly lansium domesticum peel biosorbent," *Ecotoxicology and Environmental Safety*, vol. 127, May. 2016. [Online]. Available: <https://doi.org/10.1016/j.ecoenv.2016.01.003>
- [5] V. Manirethan, N. Gupta, R. M. Balakrishnan, and K. Raval, "Batch and continuous studies on the removal of heavy metals from aqueous solution using biosynthesised melanin-coated pvdf membranes," *Environmental Science and Pollution Research*, vol. 27, Oct. 10, 2019. [Online]. Available: <https://doi.org/10.1007/s11356-019-06310-8>
- [6] S. Buxton and *et al.*, "Concise review of nickel human health toxicology and ecotoxicology," *Inorganics (Special Issue Bioinorganic Chemistry of Nickel)*, vol. 7, no. 7, May. 24, 2019. [Online]. Available: <https://doi.org/10.3390/inorganics7070089>
- [7] S. Afroze and T. K. Sen, "A review on heavy metal ions and dye adsorption from water by agricultural solid waste adsorbents," *Water, Air, & Soil Pollution*, vol. 229, no. 7, Jun. 20, 2018. [Online]. Available: <https://doi.org/10.1007/s11270-018-3869-z>
- [8] C. Lee and *et al.*, "Removal of copper, nickel and chromium mixtures from metal plating wastewater by adsorption with modified carbon foam," *Chemosphere*, vol. 116, Ene. 2017. [Online]. Available: <https://doi.org/10.1016/j.chemosphere.2016.09.093>
- [9] Y. Chen, H. Wang, W. Zhao, and S. Huang, "Four different kinds of peels as adsorbents for the removal of cd (ii) from aqueous solution: Kinetics, isotherm and mechanism," *Journal of the Taiwan Institute of Chemical Engineers*, vol. 88, Jul. 2018. [Online]. Available: <https://doi.org/10.1016/j.jtice.2018.03.046>
- [10] N. M. Rane, S. P. Shewale, S. V. Admane, and R. S. Sapkal, "Adsorption of hexavalent chromium by using sweet lime and orange peel powder," in *Novel Water Treatment and Separation Methods: Simulation of Chemical Processes*. Toronto, Waretown, NJ: Apple Academic Press, 2017, pp. 101-114.
- [11] A. ul Haq and *et al.*, "Evaluation of sorption mechanism of pb (ii) and ni (ii) onto pea (pisum sativum) peels," *Journal of Oleo Science*, vol. 66, no. 7, 2017. [Online]. Available: <https://doi.org/10.5650/jos.ess17020>
- [12] C. Tejada-Tovar, A. Villabona-Ortíz, and E. Ruiz-Paternina, "Adsorción de ni (ii) por cáscaras de ñame (dioscorea rotundata) y bagazo de palma (elaeis guineensis) pretratadas," *Revista Luna Azul [On Line]*, no. 42, Feb. 9, 2016. [Online]. Available: <https://doi.org/10.17151/luaz.2016.4>
- [13] P. Premkumar and R. Sudha, "Comparative studies on the removal of chromium(vi) from aqueous solutions using raw and modified citrus limettioides peel," *Indian Journal of Chemical Technology*, vol. 25, no. 3, 2018. [Online]. Available: <http://14.139.47.23/index.php/IJCT/article/view/11706>
- [14] S. Parlayici and E. Pehlivan, "Comparative study of cr(vi) removal by bio-waste adsorbents: equilibrium, kinetics, and thermodynamic," *Journal of Analytical Science and Technology*, vol. 10, no. 1, Abr. 6, 2019. [Online]. Available: <https://doi.org/10.1186/s40543-019-0175-3>
- [15] R. Rinaldi, Y. Yasdi, and W. L. C. Hutagalung, "Removal of ni (ii) and cu (ii) ions from aqueous solution using rambutan fruit peels (nephelium lappaceum l.) as adsorbent," *Communications*

- Week, vol. 2026, no. 1, Oct. 29, 2018. [Online]. Available: <https://doi.org/10.1063/1.5065058>
- [16] H. O. N. Altino, B. E. S. Costa, and R. N. D. Cunha, "Biosorption optimization of ni(II) ions on macauba (*acrocromia aculeata*) oil extraction residue using fixed-bed column," *Journal of Environmental Chemical Engineering*, vol. 5, no. 5, Oct. 2017. [Online]. Available: <https://doi.org/10.1016/j.jece.2017.09.025>
- [17] N. M. Rane, S. V. Admane, and R. S. Sapkal, *Adsorption of Hexavalent Chromium from Wastewater by Using Sweetlime and Lemon Peel Powder by Batch Studies*. Singapore: Springer, 2019.
- [18] H. T. Vu, C. J. Scarlett, and Q. V. Vuong, "Phenolic compounds within banana peel and their potential uses: A review," *Journal of Functional Foods*, vol. 40, Ene. 2018. [Online]. Available: <https://doi.org/10.1016/j.jff.2017.11.006>
- [19] B. C. Maniglia and D. R. Tapia-Blácido, "Isolation and characterization of starch from babassu mesocarp," *Food Hydrocolloids*, vol. 55, 2016. [Online]. Available: <https://doi.org/10.1016/j.foodhyd.2015.11.001>
- [20] C. Tejada-Tovar, A. Herrera-Barros, and E. Ruiz-Paternina, "Utilización de biosorbentes para la remoción de níquel y plomo en sistemas binarios," *Ciencia en desarrollo*, vol. 7, no. 1, Feb. 15, 2016. [Online]. Available: <https://doi.org/10.19053/01217488.4228>
- [21] Z. Mahdi, Q. J. Yu, and A. E. Hanandeh, "Investigation of the kinetics and mechanisms of nickel and copper ions adsorption from aqueous solutions by date seed derived biochar," *Journal of Environmental Chemical Engineering*, vol. 6, no. 1, Feb. 2018. [Online]. Available: <https://doi.org/10.1016/j.jece.2018.01.021>
- [22] J. Wang and X. Guo, "Adsorption kinetic models: Physical meanings, applications, and solving methods," *Journal of Hazardous Materials*, vol. 390, May. 15, 2020. [Online]. Available: <https://doi.org/10.1016/j.jhazmat.2020.122156>
- [23] H. N. Tran, S. J. You, and H. P. Chao, "Thermodynamic parameters of cadmium adsorption onto orange peel calculated from various methods: A comparison study," *Journal of Environmental Chemical Engineering*, vol. 4, no. 3, Sep. 2016. [Online]. Available: <https://doi.org/10.1016/j.jece.2016.05.009>
- [24] E. C. Nleonu, E. E. Oguzie, G. N. Onuoha, and P. I. Okeke, "The potentials of chrysophyllum albidum peels as natural adsorbent," *World Journal of Pharmaceutical Research*, vol. 6, no. 6, 2017. [Online]. Available: <http://doi:10.20959/wjpr20176-8548>
- [25] N. M. A. Al-Lagtah, A. H. Al-Muhtaseb, M. N. M. Ahmad, and Y. Salameh, "Chemical and physical characteristics of optimal synthesised activated carbons from grass-derived sulfonated lignin versus commercial activated carbons," *Microporous and Mesoporous Materials*, vol. 225, May. 1, 2016. [Online]. Available: <https://doi.org/10.1016/j.micromeso.2016.01.043>
- [26] D. Chirik and K. Louhab, "A kinetics, isotherms, and thermodynamic study of diclofenac adsorption using activated carbon prepared from olive stones," *Communications Week*, vol. 39, no. 6, 2018. [Online]. Available: <https://doi.org/10.1080/01932691.2017.1395346>
- [27] A. A. Ceyhan, O. Sahin, O. Baytar, and C. Saka, "Surface and porous characterization of activated carbon prepared from pyrolysis of biomass by two-stage procedure at low activation temperature and its the adsorption of iodine," *Journal of Analytical and Applied Pyrolysis*, vol. 104, Nov. 2013. [Online]. Available: <https://doi.org/10.1016/j.jaap.2013.06.009>
- [28] W. Cherdchoo, S. Nithetham, and J. Charoenpanich, "Removal of cr(vi) from synthetic wastewater by adsorption onto coffee ground and mixed waste tea," *Chemosphere*, vol. 221, Abr. 2019. [Online]. Available: <https://doi.org/10.1016/j.chemosphere.2019.01.100>
- [29] S. M. Batagarawa and A. K. Ajibola, "Comparative evaluation for the adsorption of toxic heavy metals on to millet, corn and rice husks as adsorbents," *Journal of Analytical & Pharmaceutical Research*, vol. 8, no. 3, May. 24, 2019. [Online]. Available: <http://doi:10.15406/japlr.2019.08.00325>
- [30] K. Johari and *et al.*, "Adsorption enhancement of elemental mercury by various surface modified coconut husk as eco-friendly low-cost adsorbents," *International Biodeterioration & Biodegradation*, vol. 109, Abr. 2016. [Online]. Available: <https://doi.org/10.1016/j.ibiod.2016.01.004>
- [31] I. A. Aguayo-Villarreal, A. Bonilla-Petriciolet, and R. Muñiz-Valencia, "Preparation of activated carbons from pecan nutshell and their application in the antagonistic adsorption of heavy metal ions," *Journal of Molecular Liquids*, vol. 230, Mar. 2017. [Online]. Available: <https://doi.org/10.1016/j.molliq.2017.01.039>
- [32] R. Labied, O. Benturki, A. Y. E. Hamitouche, and A. Donnot, "Adsorption of hexavalent chromium by activated carbon obtained from a waste lignocellulosic material (ziziphus jujuba cores): Kinetic, equilibrium, and thermodynamic study," *Adsorption Science & Technology*, vol. 36, no. 3-4, Ene. 14, 2018. [Online]. Available: <https://doi.org/10.1177/0263617417750739>
- [33] Y. Wu and *et al.*, "Functionalized agricultural biomass as a low-cost adsorbent: Utilization of rice straw incorporated with amine groups for the adsorption of cr(vi) and ni(ii) from single and binary systems," *Biochemical Engineering Journal*, vol. 105, no. Parte A, Ene. 15, 2016. [Online]. Available: <https://doi.org/10.1016/j.bej.2015.08.017>
- [34] N. A. Medellín-Castillo, M. G. Hernández-Ramírez, J. J. Salazar-Rábago, G. J. Labrada-Delgado, and A. Aragón-Piña, "Bioadsorción de plomo (ii) presente en solución acuosa sobre residuos de fibras naturales procedentes de la industria ixtlera (agave lechuguilla torr. y yucca carnerosana (trel.) mckelvey)," *Revista internacional de contaminación ambiental*, vol. 33, no. 2, May. 2017. [Online]. Available: <https://doi.org/10.20937/rica.2017.33.02.08>
- [35] S. Singh and S. R. Shukla, "Theoretical studies on adsorption of ni(ii) from aqueous solution using citrus limetta peels," *Environmental Progress & Sustainable Energy*, vol. 36, no. 3, Ene. 14, 2017. [Online]. Available: <https://doi.org/10.1002/ep.12526>
- [36] R. Sudha, K. Srinivasan, and P. Premkumar, "Removal of nickel(ii) from aqueous solution using citrus limettioides peel and seed carbon," *Ecotoxicology and Environmental Safety*, vol. 117, Jul. 2015. [Online]. Available: <https://doi.org/10.1016/j.ecoenv.2015.03.025>
- [37] W. P. Putra and *et al.*, "Biosorption of cu(ii), pb(ii) and zn(ii) ions from aqueous solutions using selected waste materials: Adsorption and characterisation studies," *Journal of Encapsulation and Adsorption Sciences*, vol. 4, no. 1, Mar. 1, 2014. [Online]. Available: <http://doi:10.4236/jeas.2014.41004>
- [38] O. Allahdin, J. Mabingui, M. Wartel, and A. Boughriet, "Removal of pb<sup>2+</sup> ions from aqueous solutions by fixed-bed column using a modified brick: (micro)structural, electrokinetic and mechanistic aspects," *Applied Clay Science*, vol. 148, Nov. 2017. [Online]. Available: <https://doi.org/10.1016/j.clay.2017.08.002>
- [39] S. Rangabhashiyam and N. Selvaraju, "Adsorptive remediation of hexavalent chromium from synthetic wastewater by a natural and zncl<sub>2</sub> activated sterculia guttata shell," *Journal of Molecular Liquids*, vol. 207, Jul. 2015. [Online]. Available: <https://doi.org/10.1016/j.molliq.2015.03.018>
- [40] H. Guedidi, L. Reinert, Y. Soneda, N. Bellakhal, and L. Duclaux, "Adsorption of ibuprofen from aqueous solution on chemically surface-modified activated carbon cloths," *Arabian Journal of Chemistry*, vol. 10, no. 2, May. 2017. [Online]. Available: <https://doi.org/10.1016/j.arabjc.2014.03.007>
- [41] M. Mushtaq, H. Nawaz, M. Iqbal, and S. Noreen, "Eriobotrya japonica seed biocomposite efficiency for copper adsorption: Isotherms, kinetics, thermodynamic and desorption studies," *Journal of Environmental Management*, vol. 176, Jul. 1, 2016. [Online]. Available: <https://doi.org/10.1016/j.jenvman.2016.03.013>
- [42] N. Renugadevi, R. Rajalakshmi, S. Subhashini, P. Lalitha, and T. Malarvizhi, "Usefulness of activated carbon prepared from agro waste in the removal of dyes from aqueous solution," *Indian Journal of Environmental Protection*, vol. 29, no. 3, Mar. 2009. [Online]. Available: <https://bit.ly/3ybCF3C>
- [43] N. Ibsi and C. Asoluka, "Use of agro-waste (musa paradisiaca peels) as a sustainable biosorbent for toxic metal ions removal from contaminated water," *Chemistry International*, vol. 4, no. 1, Ene. 2018. [Online]. Available: <http://bosajournals.com/chemint/images/pdf/18-7.pdf>
- [44] R. A. Khera and *et al.*, "Kinetics and equilibrium studies of copper, zinc, and nickel ions adsorptive removal on to archontophoenix alexandrae: conditions optimization by rsm," *Desalination and*

- Water Treatment*, vol. 201, Oct. 2020. [Online]. Available: <https://doi.org/10.5004/dwt.2020.25937>
- [45] K. M. Oghenejoboh, "Biosorption of nickel (ii) ion from synthetic wastewater on watermelon rind activated carbon using response surface methodology (rsm) optimization approach," *Nigerian Journal of Technology*, vol. 37, no. 3, Jul. 2018. [Online]. Available: <http://dx.doi.org/10.4314/njt.v37i3.13>
- [46] C. Tejada-Tovar, A. Villabona-Ortiz, A. Cabarcas, C. Benitez, and D. Acevedo, "Optimization of variables in fixed-bed column using the response surface methodology," *Contemporary Engineering Sciences*, vol. 11, no. 3, 2018. [Online]. Available: <https://doi.org/10.12988/ces.2018.83101>
- [47] Z. N. Garba, N. I. Ugbaga, and A. K. Abdullahi, "Evaluation of optimum adsorption conditions for ni (ii) and cd (ii) removal from aqueous solution by modified plantain peels (mpp)," *Beni-Suef University Journal of Basic and Applied Sciences*, vol. 5, no. 2, Jun. 2016. [Online]. Available: <https://doi.org/10.1016/j.bjbas.2016.03.001>
- [48] M. Vasudevan, P. S. Ajithkumar, R. P. Singh, and N. Natarajan, "Mass transfer kinetics using two-site interface model for removal of cr(vi) from aqueous solution with cassava peel and rubber tree bark as adsorbents," *Korean Society of Environmental Engineers*, vol. 21, no. 2, Jun. 30, 2016. [Online]. Available: <https://doi.org/10.4491/eer.2015.152>
- [49] J. Shah, M. R. Jan, A. Haq, and M. Zeeshan, "Equilibrium, kinetic and thermodynamic studies for sorption of ni (ii) from aqueous solution using formaldehyde treated waste tea leaves," *Journal of Saudi Chemical Society*, vol. 19, no. 3, May. 2015. [Online]. Available: <https://doi.org/10.1016/j.jscs.2012.04.004>
- [50] K. M. Doke and E. M. Khan, "Equilibrium, kinetic and diffusion mechanism of cr(vi) adsorption onto activated carbon derived from wood apple shell," *Arabian Journal of Chemistry*, vol. 10, no. 1, Feb. 2017. [Online]. Available: <https://doi.org/10.1016/j.arabjc.2012.07.031>
- [51] E. Bibaj and *et al.*, "Activated carbons from banana peels for the removal of nickel ions," *International Journal of Environmental Science and Technology*, vol. 16, Feb. 4, 2019. [Online]. Available: <https://doi.org/10.1007/s13762-018-1676-0>
- [52] H. Haroon and *et al.*, "Equilibrium kinetic and thermodynamic studies of cr(vi) adsorption onto a novel adsorbent of eucalyptus camaldulensis waste: Batch and column reactors," *Korean Journal of Chemical Engineering*, vol. 33, Sep. 19, 2016. [Online]. Available: <https://doi.org/10.1007/s11814-016-0160-0>
- [53] M. Šuránek, Z. Melichová, V. Kureková, L. Kljajević, and S. Nenadović, "Removal of nickel from aqueous solutions by natural bentonites from slovakia," *Materials*, vol. 14, no. 2, Ene. 7, 2021. [Online]. Available: <https://doi.org/10.3390/ma14020282>
- [54] R. M. Naik, S. Ratan, and I. Singh, "Use of orange peel as an adsorbent for the removal of cr(vi) from its aqueous solution," *Indian Journal of Chemical Technology*, vol. 25, May. 2018. [Online]. Available: <http://nopr.niscair.res.in/handle/123456789/44561>
- [55] S. Mondal, K. Sinha, K. Aikat, and G. Halder, "Adsorption thermodynamics and kinetics of ranitidine hydrochloride onto superheated steam activated carbon derived from mung bean husk," *Journal of Environmental Chemical Engineering*, vol. 3, no. 1, Mar. 2015. [Online]. Available: <https://doi.org/10.1016/j.jece.2014.11.021>